

Hydrogen Bonds and van der Waals Forces in Ice at Ambient and High Pressures

Biswajit Santra,¹ Jiří Klimeš,^{2,3,4} Dario Alfè,^{2,4,5,6} Alexandre Tkatchenko,¹ Ben Slater,^{3,4}
Angelos Michaelides,^{2,3,4,*} Roberto Car,⁷ and Matthias Scheffler¹

¹*Fritz-Haber-Institut der Max-Planck-Gesellschaft, Faradayweg 4-6, 14195 Berlin, Germany*

²*London Centre for Nanotechnology, University College London, London WC1E 6BT, United Kingdom*

³*Department of Chemistry, University College London, London WC1E 6BT, United Kingdom*

⁴*Thomas Young Centre, University College London, London WC1E 6BT, United Kingdom*

⁵*Department of Physics and Astronomy, University College London, London WC1E 6BT, United Kingdom*

⁶*Department of Earth Sciences, University College London, London WC1E 6BT, United Kingdom*

⁷*Department of Chemistry, Princeton University, Princeton, New Jersey 08544, USA*

(Received 29 July 2011; published 25 October 2011)

The first principles methods, density-functional theory and quantum Monte Carlo, have been used to examine the balance between van der Waals (vdW) forces and hydrogen bonding in ambient and high-pressure phases of ice. At higher pressure, the contribution to the lattice energy from vdW increases and that from hydrogen bonding decreases, leading vdW to have a substantial effect on the transition pressures between the crystalline ice phases. An important consequence, likely to be of relevance to molecular crystals in general, is that transition pressures obtained from density-functional theory exchange-correlation functionals which neglect vdW forces are greatly overestimated.

DOI: 10.1103/PhysRevLett.107.185701

PACS numbers: 64.70.K-, 62.50.-p, 71.15.Nc

Water ice, the most common molecular solid in nature, exhibits a rich and complex phase diagram. At present, this includes ice *Ih*, ice *Ic*, and 14 other crystalline ice phases [1,2]. Although the phase diagram of ice up to around 2 GPa is well-established experimentally, understanding of the subtle balance of intermolecular interactions which give rise to this richness is incomplete. In particular, the relative contribution of hydrogen (H) bonding and van der Waals (vdW) dispersion forces to the cohesive properties of the various crystalline ice phases is still not understood. From a theoretical perspective, the varied densities of experimentally characterized ice crystal structures, with the molecules fixed on well-defined lattices, afford an excellent opportunity to quantify and assess the nature of these intermolecular interactions.

Computer simulation techniques have proved instrumental in understanding ice (e.g., [3–14]). In particular, density-functional theory (DFT) with generalized gradient approximation (GGA) functionals has been widely applied. Certain GGAs describe the ambient pressure ice *Ih* phase reasonably well [9] and predict the proton order-disorder phase transition temperatures between ice *Ih* and XI and ice VII and VIII in good agreement with experiments [6]. However, it is known that GGAs suffer deficiencies when vdW forces are important, and indeed it has been suggested that this is the reason certain GGAs produce a liquid water density about 15–20% less than experiment [15–17] or fail to predict the correct ground state structure for some small water clusters [18]. Despite the considerable body of DFT work on ice phases, the role of vdW forces and H bonding has not been systematically examined in anything other than ice *Ih* [19–21]. However,

with recent developments (e.g., [22–24]), it is now possible to tackle this issue head-on and estimate the importance of vdW forces and H bonding in the various phases of ice.

Here, we report an extensive series of first principles studies aimed at better understanding the role of vdW and H bonding in ice. This includes DFT calculations with and without a treatment of vdW forces on the ambient pressure phase of ice, ice *Ih*, and all the proton ordered phases, namely, in order of increasing pressure: ice IX, II, XIII, XIV, XV, and VIII. We also report diffusion quantum Monte Carlo (DMC) calculations for ice *Ih*, II, and VIII as reference values to complement the experimental results. DMC calculations are highly accurate for weak interactions, including vdW-bonded systems, and represent the state of the art for electronic structure simulations of solids. In this Letter, we find that the contribution of vdW to the cohesive properties of ice increases as one moves to the higher-density phases, whereas the contribution from H bonds decreases. As a result, vdW plays a crucial role in determining the relative stabilities and phase transition pressures in ice. The results presented here are likely to be of relevance to understanding intermolecular interactions in water in all its condensed phases, as well as to structural searches for (novel) high-pressure ices and to molecular crystals in general.

The FHI-aims [25] and VASP [26,27] codes have been used for the DFT calculations; the former is an all-electron code with a numeric atom-centered orbital basis set and the latter a plane-wave basis set code with projector-augmented wave potentials. DMC calculations were performed using the CASINO [28] code within the fixed-node pseudopotential approximation (using Dirac-Fock

TABLE I. Absolute lattice energies (omitting zero-point energy effects) of ice *Ih*, II, and VIII. Relative energies compared to ice *Ih* (ΔU_0) are given in parentheses. All values are in meV/H₂O.

	<i>Ih</i>	II	VIII
Experiment ^a	-610	-609(1)	-577(33)
DMC	-605 ± 5	-609 ± 5(-4)	-575 ± 5(30)
PBE	-636	-567(69)	-459(177)
PBE0	-598	-543(55)	-450(148)
PBE0 + vdW ^{TS}	-672	-666(6)	-596(76)

^aRef. [31], with zero-point energy contributions removed.

pseudopotentials) and a *B*-spline basis set [29]. Further computational details can be found in the Supplemental Material [30].

We start by discussing lattice energies, which are obtained by subtracting the total energy of the ice unit cell containing *n* H₂O molecules from the total energy of *n* isolated H₂O molecules. In this context, Whalley's extrapolations of the experimental finite temperature and pressure phase coexistence lines to zero temperature and pressure are extremely valuable [31]. For the proton ordered phases Whalley considered, these indicate that ice IX, II, and VIII are less stable than ice *Ih* by only 3.5 ± 0.8 , 0.6 ± 1.0 , and 33 meV/H₂O, respectively [31]. These values agree well with DMC calculations. Specifically, DMC calculations predict that ice VIII is 30 ± 7 meV/H₂O less stable than ice *Ih*. Similarly, the near-energetic degeneracy between ice *Ih* and ice II is captured with DMC calculations, and, within the DMC error bars, ice *Ih* and ice II are equally stable. From Table I, it can also be seen that DMC lattice energies are in very good agreement with experiment as well. Indeed, the general agreement between DMC calculations and experiment for the ice phases considered is excellent. Overall, the DMC results confirm the success of Whalley's experimental extrapolations; hence, these taken together provide an excellent reference for exploring the role of H bonds and vdW in ice with DFT.

We now discuss the results obtained with Perdew-Burke-Ernzerhof (PBE) [32], one of the most widely used DFT functionals. For ice *Ih*, PBE yields a reasonable lattice energy of about 640 meV/H₂O, an overestimate of around 30 meV/H₂O, which is consistent with previous work [9]. However, Table I and Fig. 1(a) reveal a severe deterioration in the performance of PBE for the higher-density phases. Whereas experiment and DMC suggest that the energy difference between ice *Ih* and the least stable ice VIII phase is about 30 meV/H₂O, PBE gives ~ 180 meV/H₂O difference. This is mainly because PBE underestimates the stability of the high-pressure phases, suggesting that attractive interactions, more important in the higher-density ice phases, are not captured accurately with PBE. In addition to substantially overestimating the energy differences between the various phases, the changes in volumes (ΔV_0) upon going from ice *Ih* to the high-pressure phases are also underestimated with PBE [Fig. 1(b)], and critically the estimated transition pressures (P_{tr})—obtained from $P_{tr} = -\Delta U_0/\Delta V_0$ —are ~ 5 – 15 times larger than experiment [Fig. 1(c)].

Seeking to understand why PBE performs so poorly for the high-pressure ice phases, we considered the sensitivity of the results to Hartree-Fock exchange (HF x), H bonding, and vdW interactions. First, we analyzed the dipole moment and polarizability of an isolated water molecule. PBE, like other GGAs, overestimates the polarizability of an isolated water molecule by $\sim 10\%$ compared to experiment, which is related to an overly delocalized electron density and an underestimated energy gap between the highest occupied molecular orbital (HOMO) and the lowest unoccupied molecular orbital (LUMO). Incorporation of a fraction of HF x into the GGAs is an established approach for remedying this problem to some extent. In particular, a popular PBE-based hybrid functional, PBE0 [33], widens the HOMO-LUMO gap of the isolated water molecule by $\sim 40\%$ and provides more accurate polarizabilities and interaction energies within a variety of water clusters [34–36]. When applied to ice, the lattice energies

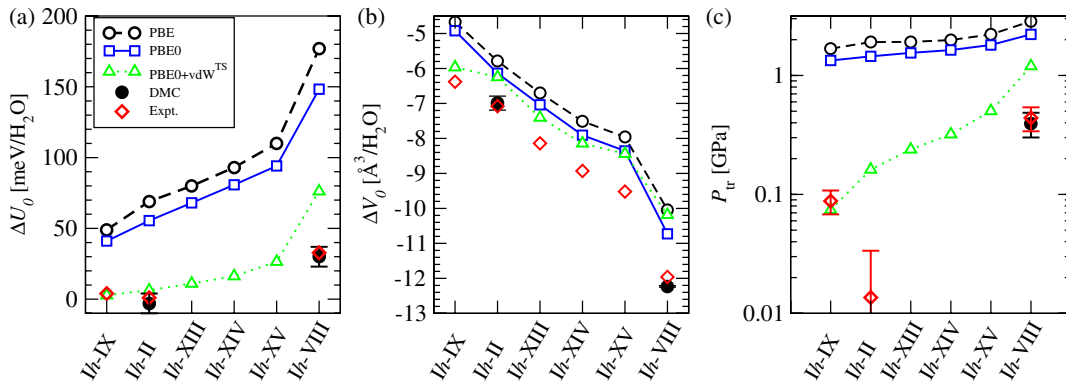


FIG. 1 (color online). (a) Relative lattice energies (ΔU_0) and (b) volumes (ΔV_0) of the high-pressure ice phases with respect to the lattice energy of ice *Ih* obtained with the methods indicated. (c) Transition pressures (P_{tr}) from ice *Ih* to the various high-pressure phases.

obtained with PBE0 (Table I) are indeed improved over PBE; however, the energy difference between ice *Ih* and ice VIII is still about 4 times larger than the experimental value. In addition, as with PBE, upon going from ice *Ih* to the high-pressure phases, the transition pressures are about an order of magnitude too large compared to experiment [Fig. 1(c)]. Note that, in addition to the 25% HFx in PBE0, other percentages of HFx are possible and have been considered. The results are sensitive to the percentage HFx used, but the errors in the relative energies of the phases persist no matter what percentage is used (Fig. S4).

Turning to the role of H bonding, the relative H bond strength has been estimated from shifts in the O-H stretching frequencies, which is a simple and widely used measure of H bond strength (e.g., [37]). Specifically, the softening (redshift) of the intramolecular O-H stretching frequencies in the various phases is compared to the (average) O-H stretching frequency of an isolated water monomer [38]. Based on the available experimental frequencies for several of the phases [39–41], H bonds get weaker with increasing pressure. This established, but not necessarily obvious, result arises because the nearest neighbor water-water distances get larger as one moves from ice *Ih* with its open ring structure to the more complex higher-pressure phases. In line with previous calculations [42], PBE reproduces the trend in frequency changes with pressure, but the redshift (i.e., strength) compared to the isolated water molecule is significantly overestimated compared to experiment, particularly for ice *Ih* [see Fig. 2(a)]. PBE0 predicts frequency shifts in much better agreement with experiment [Fig. 2(a)]. However, as we have seen, the relative stabilities of the ice phases with PBE0 are significantly in error, which clearly suggests that H bonds are not the only important interaction in the high-density phases.

We now consider the influence of vdW interactions with the scheme of Tkatchenko and Scheffler (referred to as vdW^{TS}), in which an additional C_6/R^6 tail is added to the DFT total energy, with the C_6 coefficients calculated as functionals of the electron density [23]. Dramatic

improvements in the relative energies of the various phases and phase transition pressures are observed (Fig. 1). In particular, upon going from PBE0 to PBE0 + vdW^{TS}, the energy difference between ice *Ih* and ice II is reduced to just 6 meV/H₂O, and, likewise, ice VIII is now only 76 meV/H₂O less stable than ice *Ih*. As a consequence, with vdW, the ice *Ih* to ice II transition pressure is reduced by more than 1 order of magnitude and is in good agreement with experiment. Similarly, the ice *Ih* to ice VIII transition comes within a factor of 2 of experiment. The substantially improved transition properties when vdW is accounted for result from a strong dependence of vdW on density, as shown in Fig. 2(b). Clearly, as the density of the ice phases increases, so too does the vdW contribution to the lattice energy; indeed, for the highest-density phase (ice VIII), the vdW contribution is about twice what it is in ice *Ih*. Overall, the decrease of H bond strength and the increase of vdW in the high-pressure phases clearly shows a significant enhancement of the relative contribution of vdW over H bonding interactions for the cohesive properties of the high-pressure ice phases.

Our findings regarding the importance of vdW for the high-pressure phases of ice also hold when using functionals based on the vdW-DF approach of Dion *et al.* [22,43]. The phase transition pressures obtained with such functionals are similar to those obtained with the TS scheme. Indeed, the ice *Ih* to ice VIII energy differences from the vdW-DF approaches are, at 30–40 meV/H₂O, in very good agreement with experiment [44]. Both approaches neglect the nonadditive many-body vdW energy beyond the pairwise approximation. We have found that the many-body vdW energy plays a minor role for the different phases of ice by using an extension of the TS scheme [45]. Also, we find that quantum effects based on zero-point energies play a minor role in determining the relative stabilities of the various phases. Specifically, the zero-point energies of the different phases (calculated with PBE and the harmonic approximation) differ by <10 meV/H₂O.

We now discuss why vdW interactions play a crucial role in determining the relative stabilities of the various ice phases. For any two nonbonded atoms, vdW forces result from an induced-dipole–induced-dipole interaction whose leading term varies as C_6R^{-6} . At a given R , vdW will increase if the polarizability of the atoms increases; i.e., C_6 becomes larger and/or the number density of the atoms increases. Our calculations with the TS approach show that the C_6 coefficients do indeed increase upon going from ice *Ih* to ice VIII, by 24% for H and 6% for O. However, the major effect that leads to an increase in the vdW interactions in the high-density phases is simply the higher packing of water molecules. This can be seen by comparing the O-O radial distribution functions of ice *Ih* with, e.g., ice II and ice VIII [Fig. 3(a)]. Although ice *Ih* possesses the shortest nearest neighbor O-O distances, the structure is

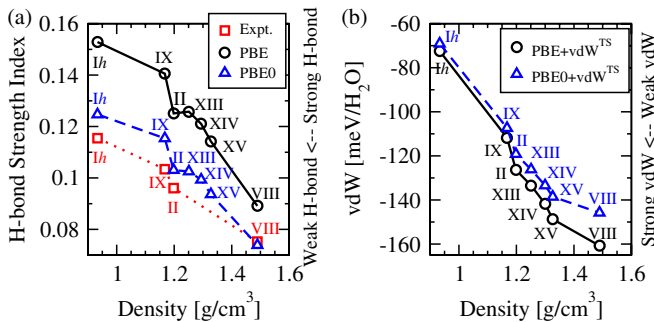


FIG. 2 (color online). (a) H bond strength index [38] and (b) vdW energy contributions plotted as a function of the experimental densities of the ice phases at zero pressure. Experimental values are taken from [39–41].

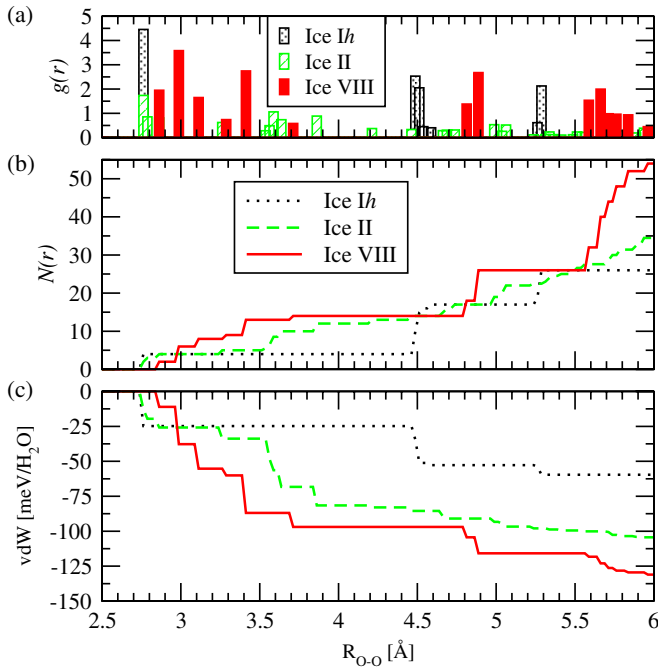


FIG. 3 (color online). (a) O-O radial distribution functions [$g(r)$] of ice *Ih*, ice II, and ice VIII. (b) Integrated number of neighbors [$N(r)$] and (c) vdW contributions (obtained from the TS scheme) as a function of O-O distance for the same three phases.

open and there is a large gap of $\sim 2 \text{\AA}$ between the first and second coordination shells. In contrast, in the high-density phases, the second and subsequent coordination shells appear at much shorter O-O separations. In fact, in ice VIII, which is comprised of two interpenetrating sublattices, the first and second coordination shells fall almost on top of each other (with the shortest O-O distances associated with non-H-bonded contacts). The higher packing, particularly in the *ca.* 3 to 6 \AA regime, is reflected by the integrated number of neighbors versus O-O distance shown in Fig. 3(b). Overall, these additional molecules at short (ice VIII) and intermediate (ice II) distances lead to enhanced vdW interactions in the high-pressure phases. Figure 3(c) provides a more quantitative basis for the above argument by showing the total vdW interactions—as obtained from the TS scheme—for ice *Ih*, II, and VIII in the range of *ca.* 3 to 6 \AA . It can be seen that, beyond about *ca.* 3 \AA , there are more substantial contributions from vdW from ice II and VIII than ice *Ih*. Although vdW is generally considered to be a long-range interaction, the dominance of vdW in this *ca.* 3 to 6 \AA regime is to be expected given that the sum of the vdW radii of O and H in the condensed phase (calculated with the TS scheme) is only $\leq 3 \text{\AA}$. Note that, in fact, the difference in the vdW contribution between the various phases is essentially converged to the periodic limit after about 8 \AA .

In conclusion, we have performed an extensive first principles study of ice at ambient and high pressures.

From the ambient to the high-pressure phases, the contribution to the lattice energy arising from vdW forces increases monotonically. This has a significant impact on the phase transition pressures, as exemplified by calculations with conventional DFT *xc* functionals where vdW forces are not accounted for and where transition pressures more than 1 order of magnitude larger than experiment are obtained. By accounting for vdW forces with DFT, the phase transition pressures more closely agree with experiment. DMC calculations, which account for vdW forces and are also free from other DFT errors such as self-interaction, offer excellent performance for the phases considered. Overall, these findings provide new physical insight and are also relevant to DFT-based structural searches for novel ice polymorphs [14,46] by implying that a reexamination of the high-pressure region of the ice phase diagram with a vdW corrected DFT approach would be worthwhile. While the focus of the current study has been on understanding the role of H bonding and vdW forces in ice, rather than on improving the current state-of-the-art in DFT simulations for water, it is nonetheless worthwhile to stress that there certainly remains scope for further improvements within DFT in terms of transition pressures, absolute lattice energies, and volumes for ice. In particular, there is scope for improving the lattice energy of ice VIII obtained with vdW^{TS} , with the current underestimation in the lattice energy possibly associated with the radically different structure of ice VIII compared to the other phases considered. The strong dependence of vdW interactions on density suggests that, even at ambient pressure, vdW forces will also be important to liquid water, which has a $\sim 8\%$ higher density than ice *Ih*. Indeed, this is consistent with a number of recent DFT studies [16,17]. Although vdW is often associated with so-called “sparse” matter, we have shown that it attains greater significance at high density. This somewhat counterintuitive result arises because vdW forces mainly enhance interactions between molecules at medium range (i.e., second and third coordination shells at 3 to 6 \AA separations). Therefore, analogous effects are expected for water in other environments such as in confined geometries, interfaces, and clathrates, and indeed for other hydrogen-bonded molecular crystals at high pressure.

A.M. is supported by the EPSRC and the European Research Council. J.K. is grateful to UCL and the EPSRC for support through the PhD+ scheme. D.A. is supported through the EURYI scheme and EPSRC. R.C. is supported by NSF Grant No. CHE-0956500. This research used resources of the Oak Ridge Leadership Computing Facility, located in the National Center for Computational Sciences at Oak Ridge National Laboratory, which is supported by the Office of Science of the Department of Energy under Contract No. DE-AC05-00OR22725. We are also grateful for computational resources to the London Centre for Nanotechnology and UCL Research

Computing as well as to the UK's HPC Materials Chemistry Consortium, which is funded by EPSRC (EP/F067496), for access to HECToR, the UK's national high-performance computing service.

*angelos.michaelides@ucl.ac.uk

- [1] C. G. Salzmann *et al.*, *Phys. Rev. Lett.* **103**, 105701 (2009) and references therein.
- [2] O. Mishima *et al.*, *Nature (London)* **314**, 76 (1985).
- [3] C. Lee *et al.*, *Phys. Rev. Lett.* **69**, 462 (1992).
- [4] D. R. Hamann, *Phys. Rev. B* **55**, R10157 (1997).
- [5] E. Sanz *et al.*, *Phys. Rev. Lett.* **92**, 255701 (2004).
- [6] S. J. Singer *et al.*, *Phys. Rev. Lett.* **94**, 135701 (2005).
- [7] G. A. Tribello, B. Slater, and C. G. Salzmann, *J. Am. Chem. Soc.* **128**, 12 594 (2006).
- [8] M. de Koning *et al.*, *Phys. Rev. Lett.* **96**, 075501 (2006).
- [9] P. J. Feibelman, *Phys. Chem. Chem. Phys.* **10**, 4688 (2008).
- [10] A. Hermann and P. Schwerdtfeger, *Phys. Rev. Lett.* **101**, 183005 (2008).
- [11] D. Pan *et al.*, *Phys. Rev. Lett.* **101**, 155703 (2008).
- [12] A. Erba *et al.*, *J. Phys. Chem. B* **113**, 2347 (2009).
- [13] J. A. Morrone *et al.*, *J. Chem. Phys.* **130**, 204511 (2009).
- [14] B. Militzer and H. F. Wilson, *Phys. Rev. Lett.* **105**, 195701 (2010).
- [15] I.-C. Lin *et al.*, *J. Phys. Chem. B* **113**, 1127 (2009).
- [16] J. Schmidt *et al.*, *J. Phys. Chem. B* **113**, 11959 (2009).
- [17] J. Wang *et al.*, *J. Chem. Phys.* **134**, 024516 (2011).
- [18] B. Santra *et al.*, *J. Chem. Phys.* **129**, 194111 (2008).
- [19] I. Hamada, *J. Chem. Phys.* **133**, 214503 (2010).
- [20] F. Labat, C. Pouchan, C. Adamo, and G. E. Scuseria, *J. Comput. Chem.* **32**, 2177 (2011).
- [21] B. Kolb and T. Thonhauser, *Phys. Rev. B* **84**, 045116 (2011).
- [22] M. Dion *et al.*, *Phys. Rev. Lett.* **92**, 246401 (2004).
- [23] A. Tkatchenko and M. Scheffler, *Phys. Rev. Lett.* **102**, 073005 (2009).
- [24] S. Grimme *et al.*, *J. Chem. Phys.* **132**, 154104 (2010).
- [25] V. Blum *et al.*, *Comput. Phys. Commun.* **180**, 2175 (2009).
- [26] G. Kresse and J. Hafner, *Phys. Rev. B* **47**, 558 (1993).
- [27] G. Kresse and J. Furthmüller, *Phys. Rev. B* **54**, 11169 (1996).
- [28] R. J. Needs *et al.*, *J. Phys. Condens. Matter* **22**, 023201 (2010).
- [29] D. Alfè and M. J. Gillan, *Phys. Rev. B* **70**, 161101 (2004).
- [30] See Supplemental Material at <http://link.aps.org/supplemental/10.1103/PhysRevLett.107.185701> for further computational details.
- [31] E. Whalley, *J. Chem. Phys.* **81**, 4087 (1984).
- [32] J. P. Perdew, K. Burke, and M. Ernzerhof, *Phys. Rev. Lett.* **77**, 3865 (1996).
- [33] C. Adamo and V. Barone, *J. Chem. Phys.* **110**, 6158 (1999).
- [34] J. R. Hammond *et al.*, *J. Chem. Phys.* **131**, 214103 (2009).
- [35] B. Santra, A. Michaelides, and M. Scheffler, *J. Chem. Phys.* **127**, 184104 (2007); **131**, 124509 (2009).
- [36] F.-F. Wang *et al.*, *J. Chem. Phys.* **132**, 134303 (2010).
- [37] X.-Z. Li, B. Walker, and A. Michaelides, *Proc. Natl. Acad. Sci. U.S.A.* **108**, 6369 (2011).
- [38] The H bond strength index is calculated as $(\nu_{\text{O-H}}^{\text{H}_2\text{O}} - \nu_{\text{O-H}}^{\text{ice}}) / \nu_{\text{O-H}}^{\text{H}_2\text{O}}$, where $\nu_{\text{O-H}}^{\text{H}_2\text{O}}$ and $\nu_{\text{O-H}}^{\text{ice}}$ are the average uncoupled covalent O-H stretching frequencies of an isolated H₂O molecule and ice, respectively. When there is no H bond, the index is zero. Frequency shifts are just one measure of relative H bond strength. Other key quantities related to H bond strength, e.g., water molecule dipole moments and covalent O-H bond lengths, also decrease from the low- to the high-density phases.
- [39] J. E. Bertie and E. Whalley, *J. Chem. Phys.* **40**, 1646 (1964).
- [40] J. E. Bertie and F. E. Bates, *J. Chem. Phys.* **67**, 1511 (1977).
- [41] P. T. T. Wong and E. Whalley, *J. Chem. Phys.* **64**, 2359 (1976).
- [42] M. V. Vener *et al.*, *Chem. Phys. Lett.* **500**, 272 (2010).
- [43] J. Klimeš, D. R. Bowler, and A. Michaelides, *J. Phys. Condens. Matter* **22**, 022201 (2010).
- [44] B. Santra *et al.* (to be published).
- [45] A. Tkatchenko *et al.* (to be published).
- [46] C. J. Pickard and R. J. Needs, *J. Chem. Phys.* **127**, 244503 (2007).